

4. Tapponnier, P., Xu, Z. Q., Roger, F., Meyer, B., Arnaud, N., Wittlinger, G. and Yang, J. S., Oblique stepwise rise and growth of the Tibet plateau. *Science*, 2001, **294**, 1671–1677.
5. Patriat, P. and Achache, J., India–Eurasia collision chronology has implications for crustal shortening and driving mechanism of plates. *Nature*, 1984, **311**, 615–621.
6. Larson, K., Burgmann, R., Bilham, R. and Freymueller, J., Kinematics of the India–Eurasia collision zone from GPS measurements. *J. Geophys. Res.*, 1999, **104**, 1177.
7. Bilham, R., Gaur, V. K. and Molnar, P., Himalayan seismic hazard. *Science*, 2001, **293**, 1442–1444.
8. Kumar, R., Gill, G. S. and Gupta, L. N., Earthquake induced structures in Pinjore Formation of Nadah area, Haryana. *J. Geol. Soc. India*, 2005, **65**, 346–352.
9. Sims, J. D., Earthquake-induced structures in sediments of the Van Norman Lake, San Fernando, California. *Science*, 1973, **182**, 161–163.
10. Scott, P. and Price, S., Earthquake induced structures in young sediments. *Tectonophysics*, 1988, **147**, 165–170.
11. McCalpin, J. P., *Paleoseismology*, Academic Press, New York, 1996, p. 588.
12. Singh, T., Structure and morphotectonics of a part of Himalayan foothills in the Morni Hills of the northern Haryana and adjoining territories of Himachal Pradesh and Chandigarh. Ph D thesis, Panjab University, Chandigarh, 2006, p. 157.
13. Mills, P. C., Genesis and diagnostic value of soft-sediment deformation structures – A review. *Sediment. Geol.*, 1983, **35**, 83–104.
14. Lowe, D. R., Subaqueous liquefied and fluidized sediment flows and their deposits. *Sedimentology*, 1976, **22**, 157–204.
15. Nocita, B. W., Soft-sediment deformation (fluid escape) features in a coarse-grained pyroclastic-surge deposit, north-central New Mexico. *Sedimentology*, 1988, **35**, 275–285.
16. Karlin, R. E. and Sally, E. B., Paleearthquake in Puget Sound region recorded in sediments from Lake Washington, USA. *Science*, 1992, **258**, 1617–1620.
17. Rosetti, D. D., Soft-sediment deformation structures in late Albian to Cenomanian deposits, Sao Luis Basin: Evidence for palaeoseismicity. *Sedimentology*, 1999, **46**, 1065–1081.
18. Obermier, S. and Pond, E. C., *Seismol. Res. Lett.*, 1999, **70**, 34–56.
19. Allen, C. R., Geological criteria for evaluating seismicity. *Geol. Soc. Am. Bull.*, 1975, **86**, 1041–1057.
20. Anand, A. and Jain, A. K., Earthquakes and deformational structure (seismites) in Holocene sediments from the Himalayan–Andaman Arc., India. *Tectonophysics*, 1987, **133**, 105–120.
21. Mohindra, R. and Bagati, T. N., Seismically induced soft sediment deformation structures (seismites) around Sumdo in Lower Spiti valley (Tethys Himalayas). *Sediment. Geol.*, 1996, **101**, 69–83.
22. Mohindra, R. and Thakur, V. C., Historic large earthquake-induced soft-sediment deformation features in the Sub-Himalayan Doon valley. *Geol. Mag.*, 1998, **135**, 269–281.
23. Sims, J. D., Determining earthquake recurrence intervals from deformational structures in young lacustrine sediments. *Tectonophysics*, 1975, **29**, 144–152.

ACKNOWLEDGEMENTS. We thank the Chairman, Centre of Advanced Study in Geology, Panjab University, Chandigarh for providing facilities. We also thank the reviewers for useful comments. Financial assistance to T.P.S. from CSIR, New Delhi in the form of Senior Research Fellowship is acknowledged.

Received 18 September 2006; revised accepted 27 June 2007

## Oxygen and carbon isotope analysis of the Miocene limestone of Kerala and its implications to palaeoclimate and its depositional setting

V. Narayanan<sup>1</sup>, S. Anirudhan<sup>1\*</sup> and Andrea G. Grottoli<sup>2</sup>

<sup>1</sup>Department of Geology, University of Kerala, Kariavattom, Thiruvananthapuram 695 581, India

<sup>2</sup>Ohio State University, School of Earth Sciences, 125 South Oval Mall, Columbus, Ohio 43210-1398, USA

**The lower Miocene to Mio-Pliocene sedimentary basin of Kerala consists of Quilon carbonate sequence (Lower–Middle Miocene), which is confined between two clastic units (Ambalapuzha and Mayyanad formations). The carbonate sequence is not extensive but restricted between Alappuzha in the north and Edava (Thiruvananthapuram district) in the south. Stable isotopic analysis on Quilon limestone for  $\delta^{18}\text{O}$  points to a warmer Miocene climate, with an average value of  $34.25^\circ\text{C}$ . This value is slightly higher than the previously estimated temperature during the Miocene. The down core decrease of  $\delta^{13}\text{C}$  values of the limestone can be correlated with the transgressive phase during which carbonate get deposited in the Tertiary sequences of Kerala, as proposed by previous workers. Bivariate plots for  $\delta^{18}\text{O}$  and  $\delta^{13}\text{C}$  reveal that the limestone forms in the field of warm-water skeletons.**

**Keywords:** Depositional setting, oxygen and carbon isotopes, palaeotemperature, Quilon limestone.

THE Tertiary sedimentary rocks of Kerala, described as the Warkallai Group of rocks, belong to the Malabar Super Groups. This group of rocks is divided into Ambalapuzha, Quilon and Mayyanad formations (Table 1). The Ambalapuzha Formation constitutes variegated sandstones, associated with white plastic clays and seams of lignite; it is considered to be a littoral facies. This facies overlaps directly over fossiliferous marine limestone, viz. the Quilon Formation. Deposition of Tertiary sediments is confined to two basins<sup>1</sup>. One is in southern Kerala, which includes exposure of Quilon Formation at sea cliffs in Pozhikkara, near Paravur and Padappakkara (Kollam District), and the others in northern Kerala (Meenkunnu, Kannur District; Figure 1). Otherwise, occurrence of Quilon limestone is reported only in the boreholes drilled between Varkala and Cherthala by the State and Central Government departments. Borehole studies<sup>2</sup> of the Varkala–Cochin sector reveal that the Quilon limestone (Lower Miocene) is encountered between Alappuzha and Kollam, and is absent in boreholes further north of Alappuzha.

\*For correspondence. (e-mail: sap5354@rediffmail.com)

# RESEARCH COMMUNICATIONS

**Table 1.** Geological classification for the Tertiary sequences of Kerala after Raha *et al.*<sup>4</sup>. Stratum studied is marked in bold font

		Lithology	Age
MALABAR SUPER GROUP	Vembanad Formation	Marine and estuarine sands, peat beds	Quaternary
	Unconformity	Laterite	
	<b>W</b> Ambalapuzha Formation	Pebbly and coarse sand with peat and variegated and mottled clay. Alteration of sand and streaky clay often with lignitic bands	Mio-Pliocene
	<b>A</b> (3–140 m)		
	<b>R</b>		
	<b>K</b> <b>Quilon Formation</b>	<b>Fossiliferous limestone with bands of calcareous clay and sand in various proportions</b>	<b>Lower–Middle Miocene</b>
	<b>A</b> <b>(0.5–130 m)</b>		
	<b>L</b> Mayyanad Formation	Coarse-to-medium-grained sandstone with interbedded white clay and lignite beds. Facies grades to sand clay alterations with lignitic bands towards the central part of the basin.	Lower Miocene
	<b>L</b> (1–270 m)		
	<b>A</b>		
<b>I</b>			
<b>G</b> Unconformity	Conglomerate horizon		
<b>R</b> Karuchal Formation (2–20 m)	Hard to compact ferruginous sandstone and clay.		
<b>O</b> Unconformity	Bauxite and lateritic horizons		
<b>U</b>	Basement (Gneisses, charnockites, leptynites etc.)		
<b>P</b>			

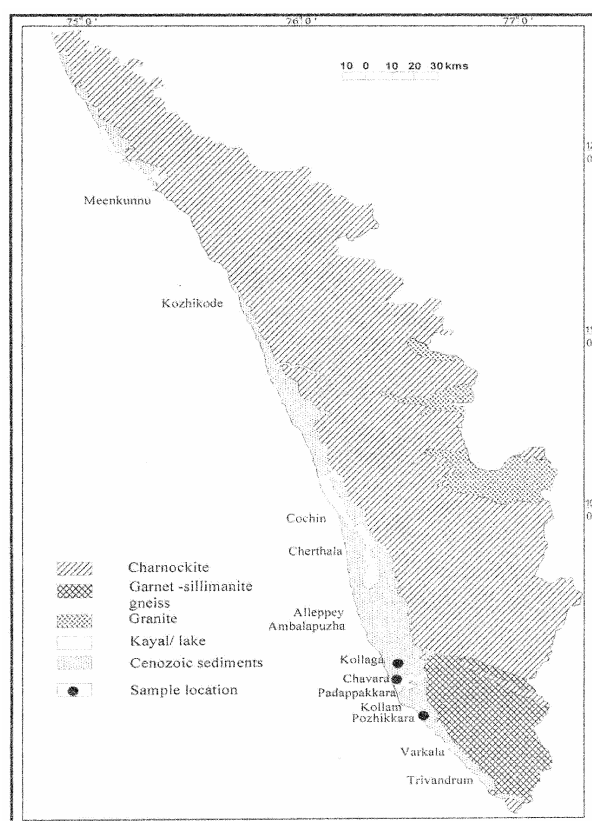


**Figure 1.** Sample locations and geology of Kerala.

Lithostratigraphic classification<sup>3,4</sup> of the basin indicates that the calcareous facies formed as result of restricted marine transgression and regression in the central part of the basin (Table 1). During the transgression period, clastics continued to deposit along the periphery of the basin. This formation, with calcareous clay, limestone and sand-

stone, gives rise to a prominent horizon with a maximum thickness of about 130 m at Ambalapuzha and around 100 m at Chavara<sup>3</sup>.

The age assigned to each formation is based on the palaeontological studies of Quilon Formation<sup>2</sup>. Palynological studies<sup>5</sup> of the Quilon limestone show that it is of Lower to Middle Miocene age. The limestone was deposited in neritic, shallow marine to brackish water conditions during the Neogene. The climate during Neogene was not much different from the present climate<sup>5</sup>. Identification of new taxa of Ostracods and isolated occurrences of shark teeth along the Quilon beds reveal an age of Lower Miocene<sup>6,7</sup>. An echinoid fossil, *Lovenia forbesi* has been reported<sup>8</sup> from a dug-out well section at Edava, Kerala. The age of the fossil is from Eocene to Recent. Authigenic minerals of Quilon limestone include pyrite and glauconite<sup>9</sup>. Glauconite and pyrite are deposited in a locally reducing environment prevalent below the sediment–water interface.

Stable isotopic analysis for <sup>18</sup>O and <sup>13</sup>C has been applied here to interpret the palaeoclimate, palaeotemperature and the processes responsible for the deposition of Quilon limestone during Lower–Middle Miocene. Limestone samples from the boreholes of Chavara (lat. 8°59'39" and long: 76°34'10") and Kollaga (lat. 9°02'51" and long. 76°32'48"), and a marl sample from the cliff sections exposed at Pozhikkara (lat. 8°49' and long. 76°40'; Figure 1) were treated for carbon and oxygen isotope studies.  $\delta^{18}\text{O}$  isotopic record of bulk carbonate from whole rock of DSDP sites 525 and 528 from the Atlantic was nearly identical to that observed in the foraminifera (benthic and planktonic)<sup>10</sup> from the other DSDP sites. The stable oxygen isotope composition ( $\delta^{18}\text{O}$ ) of a precipitated carbonate depends mainly on the isotope composition, salinity and temperature of the host fluid, whereas the stable carbon isotope composition ( $\delta^{13}\text{C}$ ) reflects the source of CO<sub>2</sub> for precipitation, such as meteoric or sea water, shell dissolution, or various biochemical origins, including microbial

**Table 2.** Stable isotope values of  $\delta^{18}\text{O}_{\text{V-PDB}}$  and  $\delta^{13}\text{C}_{\text{V-PDB}}$  for selected borehole samples of Quilon Formation, Kerala

Location	$\delta^{18}\text{O}_{\text{V-PDB}}$	$\delta^{13}\text{C}_{\text{V-PDB}}$	Temperature ( $^{\circ}\text{C}$ )	Z	Lithology	Depth down hole (m)
Kollaga	-3.98	0.825	33.56	127.01	Limestone	-45.72
Kollaga	-3.76	-0.706	32.48	123.98	Limestone	-73.15
Kollaga	-4.19	-3.044	34.54	118.98	Limestone	-91.44
Kollaga	-3.92	-2.055	33.26	121.14	Limestone	-106.68
Chavara	-4.15	-0.841	34.36	123.51	Limestone	-36.57
Chavara	-4.56	-2.094	36.31	120.74	Limestone	-64.08
Chavara	-4.69	-4.166	36.92	116.43	Limestone	-85.34
Pozhikkara	-3.77	1.286	32.55	128.06	Marl	Cliff section
Average	-4.13	-1.349	34.25	122.48		
SD	0.85	1.74	1.64	3.94		

oxidation of organic matter and methane<sup>11-14</sup>. The oxygen isotopic composition of calcium carbonate precipitated from natural water depends upon the isotopic composition of the aqueous phase and also upon temperature<sup>12</sup>. Rainwater, derived by evaporation of sea water, is depleted in  $\delta^{18}\text{O}$  and hence has negative  $\delta^{18}\text{O}$  values: a composition shared by near-surface groundwaters that have been directly derived from rainwater. Brines that are the residues of evaporation of normal sea water are enriched in heavy  $\delta^{18}\text{O}$  and have positive  $\delta^{18}\text{O}$  values.

A 160 g aliquot of each sample was acidified with 100% ortho-phosphoric acid in an automated Kiel carbonate device, and the  $\delta^{13}\text{C}$  and  $\delta^{18}\text{O}$  values of the resulting  $\text{CO}_2$  were measured in a Finnigan MAT 252 triple-collecting mass spectrometer at AGG's laboratory in the Ohio State University, USA. Location of the sampling site was determined by Global Positioning System. Sampling was carried out at selected intervals. All isotope values were reported as per mil deviation relative to V-PDB (Vienna Peedee Belemnite Limestone). At least 20% of all measurements was made in duplicate. The standard deviation of the mean for repeated analyses of NBS-19 carbonate standard ( $n = 21$ ) was  $\pm 0.04$  for  $\delta^{13}\text{C}$  and  $\pm 0.07$  for  $\delta^{18}\text{O}$ .

$\delta^{18}\text{O}$  values of the carbonate samples were more or less uniform both down core and between the boreholes. The values for  $\delta^{18}\text{O}$  range from -4.69 to -3.76‰ with an average value of -4.13‰ (Table 2). The average temperature estimated is 34.25 $^{\circ}\text{C}$ , with a maximum of 36.92 $^{\circ}\text{C}$  for the sample from Chavara borehole (-116.43 m). The minimum calculated temperature is 32.48 $^{\circ}\text{C}$  for the sample from Kollaga borehole (-73.15 m).

The palaeotemperature is estimated based on the following equation<sup>15,16</sup>:

$$T = 16.998 - 4.52(\delta_c^{18}\text{O} - \delta_w^{18}\text{O}) + 0.03(\delta_c^{18}\text{O} - \delta_w^{18}\text{O})^2, \quad (1)$$

where  $T$  is the palaeotemperature in  $^{\circ}\text{C}$ ,  $\delta_c^{18}\text{O}$  the oxygen isotopic composition of the sample (V-PDB) and  $\delta_w^{18}\text{O}$  the oxygen isotopic composition of sea water (SMOW) at the time of limestone precipitation. The Miocene composition of sea water ( $\delta_w^{18}\text{O}$ ) has been estimated<sup>15,17</sup> as -0.4‰.

$\delta^{13}\text{C}$  shows a decrease in values from top to bottom (-0.841‰ to -4.166) and (0.825‰ to -2.055‰) for Chavara and Kollaga boreholes respectively (Table 2). The maximum value of  $\delta^{13}\text{C} = 1.286$ ‰, is for the sample of marl that is exposed at Pozhikkara cliff section.

Depositional settings of the limestone can be inferred by the following equation<sup>18</sup>

$$Z = a(\delta_c^{13}\text{C} + 50) + b(\delta_w^{18}\text{O} + 50), \quad (2)$$

where  $a = 2.048$ ,  $b = 0.498$ .  $\delta_w^{18}\text{O}$  is the oxygen isotopic composition of the sample (V-PDB), and  $\delta_c^{13}\text{C}$  the carbon isotopic composition of the sample (V-PDB).

Limestone with  $Z$  values above 120 would be classified as marine, those with values below 120 as freshwater types, and those with  $Z$  values near 120 as intermediate<sup>19</sup>. Only two samples exhibit values for freshwater types (Table 2), one sample from Chavara borehole (-85.34 m) with  $Z$  value of 116.43 and another from Kollaga borehole (-91.44 m) with  $Z$  value of 118.98.

The  $\delta^{18}\text{O} - \delta^{13}\text{C}$  plots (Figure 2)<sup>19</sup> reveal that most of the samples, except one from Kollaga borehole (-45.72 m) and the marl sample from Pozhikkara cliff section, fall in the field of warm-water skeletons and overlap with the field of meteoric cements. The above two samples fall in the field of marine limestone. Values close to the point  $R$  indicate that the limestone was formed by solution precipitation from water<sup>19</sup>.

Stable oxygen isotope analysis (Table 2) revealed a higher sea surface temperature (SST) (average 34.25 $^{\circ}\text{C}$ ). It is established that the Miocene was marked by a warmer climate<sup>20,21</sup>. It is to be noted that the Himalayan orogeny, initiated during early Eocene (38 Myr), and other major geological events that followed from early Miocene (20-17 Myr) to Late Miocene, were the continuation of the Himalayan orogeny, the vast expansion of the west Antarctic ice sheet and the establishment of monsoonal circulation<sup>16</sup>. Variations in Cenozoic climate are explained by Himalayan tectonics, periodic cycles driven by orbital processes and abrupt transient climate changes<sup>22-24</sup>.

Based upon the isotopic composition of foraminiferal assemblages, SST for the Indian Ocean during Early Mio-

cene was reported<sup>15</sup> to be 30°C, while the SST for Middle Miocene was 27–29°C. These temperatures are similar to the modern SSTs. Generally, the climate during Lower to Middle Miocene was warmer compared with the overall cooling trend for the Cenozoic era<sup>17</sup>. During this period the Indian Plate had just completely crossed the equator<sup>25</sup>. The calculated SSTs (Table 2) are greater than the present-day low latitude oceans by about 4–5°C. Further, bivariate plot between  $\delta^{18}\text{O}$  and  $\delta^{13}\text{C}$  isotopes of all samples, except two, falls in the field of warm-water skeletons (Figure 2).

$\delta^{13}\text{C}$  values of both the borehole samples show an increasing trend (Table 2) from bottom to top (i.e. –4.16‰ to –0.841‰ for Chavara borehole and –2.05‰ to 0.825‰ for Kollaga borehole). Limestone deposition could be explained by invoking a transgression – regression model<sup>3</sup>. During transgression, more organic matter is locked in the marginal areas, resulting in the enrichment of  $\delta^{13}\text{C}$ , while during the regressive phase of the sea, the locked-up organic matter is eroded and oxidized, resulting in the enrichment of  $\delta^{13}\text{C}$  in the deep ocean<sup>18,26</sup>. The samples are represented by moderately low negative values to slightly positive values for  $\delta^{13}\text{C}$ . The consistent upward increase in  $\delta^{13}\text{C}$  values of samples can be correlated with the transgressive phase during which limestones get deposited. It may be noted that transgression – regression is the prevalent model for the origin of Quilon limestone<sup>3,9</sup>. Further, moderately

high values of  $\delta^{13}\text{C}$  also indicate that the limestone samples were not subjected to a major degree of diagenesis<sup>26</sup>.

Stable isotope analysis of  $\delta^{18}\text{O}$  and  $\delta^{13}\text{C}$  was used to establish the palaeotemperature of Lower–Middle Miocene of Quilon limestone that forms as a calcareous wedge-shaped deposit, sandwiched between the underlying clastic Mayyanad and the overlying clastic Warkallai formations. Such a deposit is formed during the transgressive phase, as is evident from  $\delta^{13}\text{C}$  data. The high temperature indicated by  $\delta^{18}\text{O}$  values suggests that the Miocene was generally marked by warmer climate.

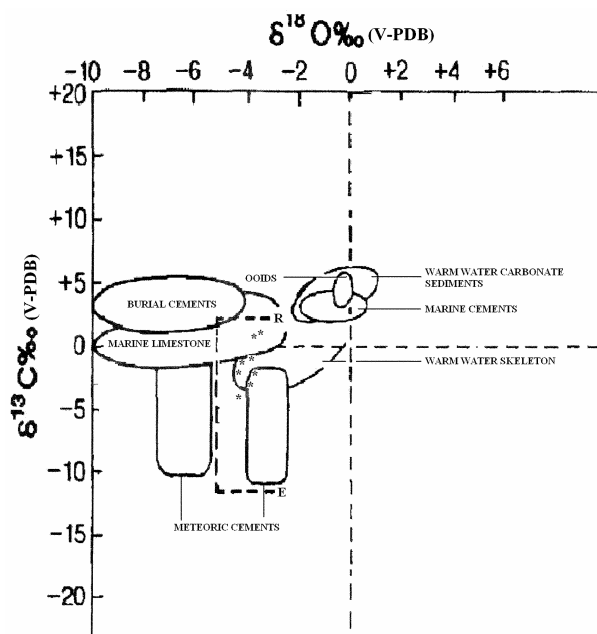


**Figure 2.** Bivariate plots of  $\delta^{18}\text{O}$ – $\delta^{13}\text{C}$  showing various isotopic fields (after Nelson and Smith<sup>19</sup>) of a selection of carbonate components. Analysed values are represented by the symbol '\*'. Heavy dashed vertical line corresponds to the meteoric calcite line to evaporation (towards E) and increasing rock–water interaction (towards R).

1. Paulose, K. V. and Narayanaswamy, S., Tertiaries of Kerala coast. *Geol. Soc. India, Mem.*, 1968, **2**, 300–308.
2. Nair, K. M. and Rao, M. R., Stratigraphic analysis of Kerala Basin. *Geol. Surv. India, Spec. Publ.*, 1980, **5**, 1–8.
3. Raha, P. K., Sinha Roy, S. and Rajendran, C. P., A new approach to the lithostratigraphy of the Cenozoic sequence of Kerala. *J. Geol. Soc. India*, 1983, **24**, 325–342.
4. Raha, P. K., A revision of the stratigraphic sequences of coastal sedimentary basin of Kerala. In *XIV Indian Colloquium Micropaleontology Stratigraphy* (eds Pandey, J. et al.), 1996, pp. 805–810.
5. Rao, K. P. and Ramanujam, C. G. K., A palynological approach to the study of Quilon beds of Kerala State in South India. *Curr. Sci.*, 1975, **44**, 730–732.
6. Khosla, S. C. and Nagoori, M. L., Ostracoda from the Quilon beds (Lower Miocene) of Kerala. *Mem. Geol. Soc. India*, 1989, **14**, 1–57.
7. Mehrotra, D. K., On the occurrence of fish remains from the Quilon beds of Kerala coast. *J. Geol. Soc. India*, 1982, **23**, 408–410.
8. Padmalal, D. and Seralathan, P., Record of fossil Echinoid, *Lovenia forbesi*, from the subsurface Quilon beds (Lower Miocene), Kerala. *J. Zool. Soc. Kerala*, 1991, **1**, 82–85.
9. Thirivikramaji, K. P. and Ghosh, S. K., Significance and genesis of early diagenetic glauconite – pyrite assemblage in the Quilon limestone, Kerala. *J. Geol. Soc. India*, 1982, **24**, 303–310.
10. Williams, F. W., Lerche, I. and Full, W. E., *Isotope Chronostratigraphy, Theory and Method*, Academic Press Geology Series, Academic Press, San Diego, 1988, p. 342.
11. Friedman, I. and O'Neil, J. R., Compilation of stable isotope fractionation factors of geochemical interest. *US Geol. Survey, Prof. Pap.*, 1977, **440K**, 12.
12. Leeder, M. R., *Sedimentology*, Chapman and Hall, London, 1982, p. 344.
13. Shackleton, N. J., *Oxygen Isotope Evidence for Cenozoic Climatic Change, Fossils and Climate* (ed. Brenchley), John Wiley, New York, 1984, pp. 27–35.
14. Rankamma, K., *Progress in Isotope Geology*, John Wiley, New York, 1963, p. 705.
15. Duncan, R. M., Stewart, A., Pearson, P. N., Ditchfield, P. W. and Singano, J. M., Miocene tropical Indian Ocean temperatures: Evidence from three exceptionally preserved foraminiferal assemblages from Tanzania. *J. Afr. Earth Sci.*, 2004, **40**, 173–190.
16. James, C. Z., Lowell, D. S. and Lohmann, K. C., Evolution of Early Cenozoic marine temperatures. *Paleoceanography*, 1994, **9**, 353–387.
17. Lear, C. H., Elderfield, P. A. and Wilson, P. A., Cenozoic deep – sea temperatures and global ice volumes from Mg/Ca in benthic foraminiferal calcite. *Science*, 2000, **287**, 269–272.
18. Madhavaraju, J., Kolosov, I., Armstrong, J. S., Ramasamy, S. and Mohan, S. P., Carbon and oxygen isotopic signatures in Albian–Danian limestones of Cauvery Basin, southeastern India. *Gondwana Res.*, 2004, **7**, 527–537.
19. Nelson, C. S. and Smith, A. M., Stable oxygen and carbon isotope compositional fields for skeletal and diagenetic components in

- New Zealand Cenozoic nontropical carbonate sediments and limestones: A synthesis and review. *N.Z. J. Geol. Geophys.*, 1996, **39**, 93–107.
20. Retallack, G. J., Carbon dioxide and climate over the past 300 Myr. *Philos. Trans. R. Soc. London*, 2002, **360**, 659–673.
  21. Retallack, G. J., A 300-million-year old record of atmospheric carbon dioxide from fossil plant cuticles. *Nature*, 2001, **360**, 287–290.
  22. James, C. Z., Mark, P., Lisa, S., Ellen, T. and Billups, K., Trends, rhythms, and aberrations in global climate 65 Ma to Present. *Science*, 2001, **292**, 686–693.
  23. James, C. Z., Michael, P. A., Timothy, J. B. and Howard, J. S., Tropical temperatures in greenhouse episodes. *Nature*, 2002, **419**, 897–898.
  24. Flower, B. P., James, C. Z. and Paul, H., Milankovitch-scale climate variability recorded near the Oligocene/Miocene boundary. In Proceedings of Ocean Drilling Program, 1997, **154**, 433–439.
  25. Prasad, C. V. R. K., *Elementary Exercises in Geology*, Universities Press (India) Pvt Ltd, 2005, p. 198.
  26. Hudson, J. D., Stable isotopes and limestone lithification. *J. Geol. Soc. London*, 1977, **133**, 637–660.

**ACKNOWLEDGEMENTS.** We acknowledge the critical suggestions and support given by Dr K. P. Thiruvikramaji. We thank Kerala State Ground Water Board for providing borehole samples.

Received 29 January 2007; revised accepted 22 August 2007

## Analyses of climatic changes around Perambikulam, South India, based on early wood mean vessel area of teak

Amalava Bhattacharyya<sup>1,\*</sup>, Dieter Eckstein<sup>2</sup>, Santosh K. Shah<sup>1</sup> and Vandana Chaudhary<sup>3</sup>

<sup>1</sup>Birbal Sahni Institute of Palaeobotany, 53, University Road, Lucknow 226 007, India

<sup>2</sup>University of Hamburg, Department of Wood Science, Division Wood Biology, Leuschnerstr 91, D-21031 Hamburg, Germany

<sup>3</sup>Department of Science and Technology, New Mehrauli Road, New Delhi 110 016, India

**Mean vessel area of early wood (EW) calculated through image analysis from dated tree-ring series of teak (*Tectona grandis* L.) at Perambikulam, Kerala has been analysed to understand its relationship with the temporal variation of climate. This study shows that rainfall during October and November (northeast monsoon) of the previous year and April of the current year is the most important climatic variable in developing the EW vessel of an annual ring. Based on this tree ring parameter, the northeast monsoon of this region has been reconstructed, which extends from AD 1743 to 1986.**

**Keywords:** Climate change, early wood, mean vessel area, teak.

VESSEL (pipe-like structure), a constituent of xylem, is primarily meant for the conduction of water from soil to leaves especially in hard wood. Its size, number, distribution in a tree ring, of both early wood (WE) and late wood (LW) portions, or in the entire ring have been recognized as significant parameters in ecology and environmental studies<sup>1–4</sup>. However, except a few from the tropical region<sup>5–7</sup>, application of vessel parameters in these aspects has been assessed mostly from temperate and Mediterranean hard wood<sup>1–3,8</sup>. Though a large number of tropical hard wood trees are known to produce growth rings<sup>9–15</sup>, only a few taxa among these seem to have the characteristic, whereby tree-ring sequences are datable exactly to their year of formation<sup>15</sup>. Teak has been widely analysed and is suitable for environmental and climatic analysis<sup>16–21</sup>. However, all these studies are based on its ring width, with the exception of one from northern Thailand, where vessel parameters have been considered<sup>5</sup>.

In this communication an attempt has been made to analyse any significant relationship existing between climate and mean vessel area (MVA) of EW of teak measured through image analysis and its prospect for climatic reconstruction from Perambikulam, Kerala, where both the southwest (SW) and northeast (NE) monsoons are prominent.

Teak samples for the present study were collected from the study area (10°20'–10°26'N lat; 76°35'–76°50'E long.), located in the southern part of the peninsular region of India (Figure 1). Based on the records of six years' climatic data (1991–96), it has been noted that average annual rainfall in this area ranges from 140.0 to 236.6 mm, with

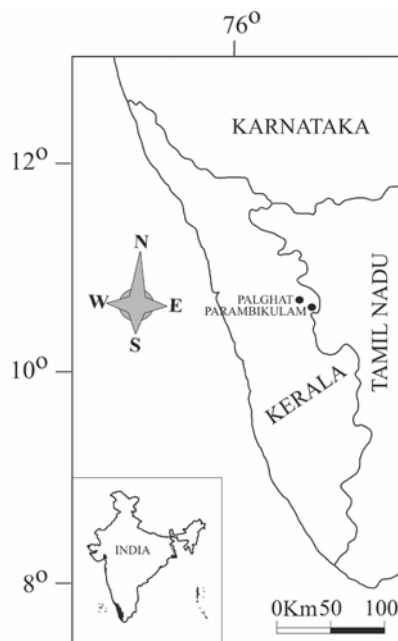


**Figure 1.** Location of tree-ring sampling site and meteorological station used in the study.

\*For correspondence. (e-mail: amalava@yahoo.com)